THREE-DIMENSIONAL ROTATIONAL ANGIOGRAPHIC DETECTION OF IN-STENT STENOSIS IN WIDE-NECKED ANEURYSMS TREATED WITH A SELF-EXPANDING INTRACRANIAL STENT

Daniel A. Hoit, M.D., M.P.H.

Cerebrovascular and Endovascular Division, Department of Neurosurgery, Tufts-New England Medical Center, and Tufts University School of Medicine, Boston, Massachusetts

Adel M. Malek, M.D., Ph.D.

Cerebrovascular and Endovascular Division, Department of Neurosurgery, Tufts-New England Medical Center, and Tufts University School of Medicine, Boston, Massachusetts

Reprint requests:
Adel M. Malek, M.D., Ph.D.
Cerebrovascular and Endovascular Division,
Department of Neurosurgery,
Tufts-New England
Medical Center,
750 Washington Street, Proger 7,
Boston, MA 02111.
Email: amalek@tufts-nemc.org

Received, December 10, 2004
Accepted, July 18, 2005

OBJECTIVE: To determine the effect of Neuroform stent (Boston Scientific/Target, Fremont, CA) deployment on parent vessel lumen and detect in-stent changes in patients harboring wide-necked intracranial aneurysms treated with the stent-coil technique.

METHODS: Parent vessel dimensions were quantified before and after the procedure and at intermediate follow-up examinations by use of high-resolution three-dimensional rotational angiography. By use of shaded surface segmentation of the acquired volume, measurements of the parent vessel proximal to the stent (Point A), at three points within the stented vascular segment (Points B, C, and D), and distal to the stent (Point E) at each study time were compared by use of paired *t* tests. Correlation between degree of in-stent stenosis and reported ischemic events was estimated by use of a linear regression model.

RESULTS: Stent and coil deployment had no immediate effect on parent vessel dimensions. At angiographic follow-up, there was no significant change in vessel size proximal to the stent. Within the stent and distal to it, however, there was a statistically significant 0.31- to 0.41-mm reduction in average diameter ($P < 0.001$, $P < 0.011$, $P < 0.003$, and $P < 0.014$ for Points B, C, D, and E, respectively). The highest degree of stenosis occurred at Point B, with an average decrease in cross sectional surface area of 2.4 mm^2 ($P < 0.001$), corresponding to a 19% stenosis and 52% estimated increase in focal hemodynamic resistance by Poiseuille's law. No clinical correlation was noted with the degree of in-stent stenosis.

CONCLUSION: Intracranial stenting using a soft self-expanding stent without angioplasty induced a statistically, but not clinically, significant decrease in cross sectional area. Further research and longer-term follow-up are needed to elucidate the mechanism and clinical importance of this response.

KEY WORDS: Anatomic constriction, Intracranial aneurysm, Intracranial thrombosis, Pathological conditions, Prostheses and implants/stent, Vascular intima

Neurosurgery 57:1228-1236, 2005 DOI: 10.1227/01.NEU.0000186026.12709.BC www.neurosurgery-online.com

The Neuroform intracranial stent (Boston Scientific/Target, Fremont, CA) is a soft, self-expanding nitinol stent designed for stent-coil treatment of wide-necked intracranial aneurysms. In contrast to previously used coronary balloon-mounted stents, the Neuroform stent is easier to navigate through tortuous segments of the cerebral vasculature and has enabled the treatment of aneurysms in previously unreachable vascular segments (2, 7, 14, 36). The performance of the Neuroform stent has been found to be competitive with other adjunctive coil-assist methods with respect to perioperative morbidity and mortality and rates of aneurysm obliteration and recanalization (2, 7, 14, 36). Despite these advantages, little is known about the long-term interaction of the stent with the parent vessel wall. Although deployment of the Neuroform stent does not involve balloon angioplasty, which may be injurious to the vessel wall (28), the long-term development of caliber changes has not yet been evaluated because of the paucity of high-resolution angiographic follow-up (22).

Copyright © Congress of Neurological Surgeons. Unauthorized reproduction of this article is prohibited.

Recent advances in three-dimensional digital rotational angiography (3D-DRA) have made possible the accurate modeling and measurement of vasculature geometry and lumen caliber. Coupled with surface reconstruction and segmentation algorithms, 3D-DRA has overcome the limitations of biplane digital subtraction angiography (2D-DSA) with regard to consistently obtaining optimal orthogonal projection for quantitative analysis (1, 4, 5, 32).

Here, we use 3D-DRA coupled with submillimeter morphometric analysis to define the angiographic response of the parent vessel in a cohort of patients undergoing Neuroform stent-coiling for treatment of wide-necked intracranial aneurysms.

PATIENTS AND METHODS

Patient Selection

In a 12-month period beginning on June 1, 2003, 18 patients harboring 19 intracranial aneurysms underwent Neuroform stent-mediated coiling of wide-necked aneurysms by the senior author. Prospective clinical data were maintained on the occurrence of transient neurological ischemic events, cerebral infarction, and assessment of neurological outcome. Fourteen patients underwent high-resolution pretreatment and posttreatment and delayed follow-up 3D-DRA and were accordingly included for analysis in this study.

Neuroform Stent-Coil Procedure

All patients in this study underwent elective treatment under general endotracheal anesthesia and were administered an antiplatelet regimen consisting of Plavix 75 mg/d (clopidogrel bisulfate, Bristol-Myers Squibb/Sanofi Pharmaceuticals, New York, NY) and aspirin 325 mg/d (acetylsalicylic acid) beginning at least 3 days before intervention. A baseline activated clotting time was obtained at the start of the procedure, and a weight-based bolus of intravenous heparin (70 U/kg) was administered after bifemoral arterial access had been obtained and before guide-catheter placement to achieve a target activated clotting time of greater than 240 seconds for the duration of the procedure. A 300-cm exchange length 0.014-inch microwire (Transend; Boston Scientific Inc., Natick, MA, or X-Celerator; Micro Therapeutics Inc., Irvine, CA) was used to access the distal cerebral parent vessel and served as the platform to advance the Neuroform stent delivery microcatheter (Boston Scientific Inc.) across the target lesion. The target aneurysm was accessed by use of a steam-shaped 150-cm 0.010-inch or 0.014-inch microcatheter (Excel 14 or SL-10; Boston Scientific Inc.). With the microcatheter in position, platinum Guglielmi detachable coils were deployed into the aneurysm (Boston Scientific Inc.) and, after a satisfactory position had been confirmed, detached by use of the electrolytic mechanism according to the manufacturer's recommendations.

3-D Modeling and Quantitative Vascular Measurement

All patients underwent high-resolution 3D-DRA before and immediately after stent and coil deployment and again at delayed follow-up on a calibrated Philips Integris Allura biplane system (Philips Medical Systems, Andover, MA). Biplane 2D-DSA and 3D-DRA imaging were performed in each case to assess for any branch occlusion, thrombus formation, degree of aneurysmal occlusion, and stent position.

The 3D-DRA data set was visualized by use of the Philips Integris 3D-RA software package (Version 2.0) on a Silicon Graphics workstation running the Irix 6.5 operating system (Silicon Graphics Inc., Mountain View, CA). All data sets were analyzed by use of the same technique. The data set was rendered first using the shaded volume setting to enable proper adjustment of threshold, and the volume was then segmented to a 3D surface for analysis (*Fig. 2*). The resulting 3D surface representing the angiographic lumen of the parent vessel and aneurysm was then oriented to obtain the optimal projection. A virtual cut plane was then used in the 3D space to section the vessel perpendicular to its major flow axis,

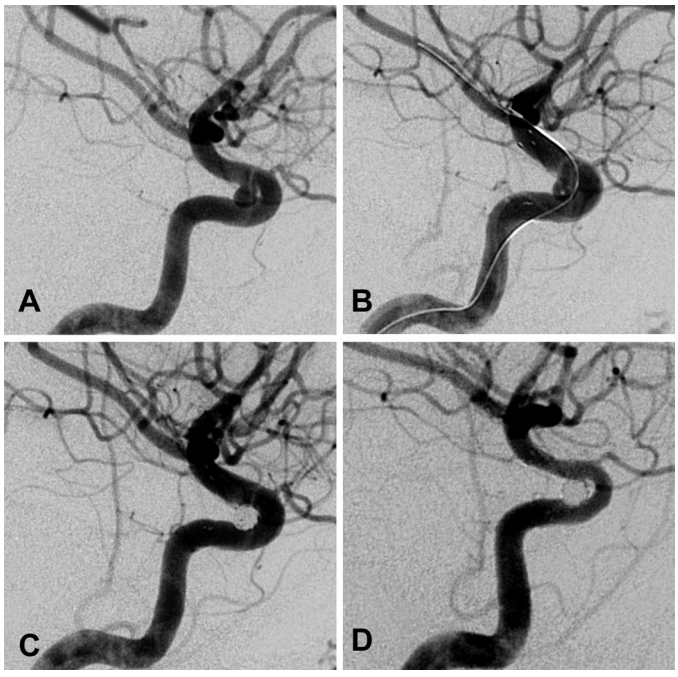


FIGURE 1. *Angiograms showing development of parent vessel remodeling after Neuroform-mediated stent-coil embolization of a wide-necked paraclinoid aneurysm.* A, *lateral view of the left internal carotid artery demonstrating a 3.5 × 3.5-mm aneurysm with a 3-mm neck.* B, *a Neuroform stent is advanced over a microguidewire and deployed with the proximal stent struts in the cavernous internal carotid artery segment and the distal stent struts positioned in the supraclinoid segment.* C, *coil embolization is performed immediately after stent deployment, with complete obliteration of the aneurysm. No change in the caliber of the parent vessel is seen after stent deployment or coil embolization.* D, *follow-up angiogram at 4 months demonstrating persistent occlusion of the aneurysm, but also de novo in-stent stenosis and restriction of the parent vessel lumen.*

Copyright © Congress of Neurological Surgeons. Unauthorized reproduction of this article is prohibited.

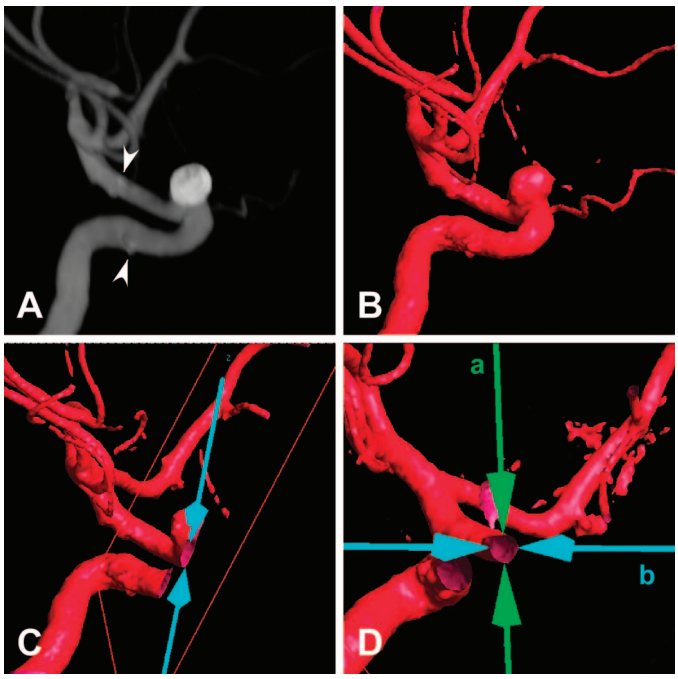


FIGURE 2. *Quantitative analysis of the 3D model of the parent vessel.* A, *volume rendering of the rotational volume data set is first generated by use of default modeling thresholds.* B, *the volume rendering is segmented to a shaded surface representing the angiographic lumen of the parent vessel.* C, *by use of a virtual cut plane, it is possible to measure the major and minor dimensions of the parent vessel orthogonal to the flow axis at multiple points.* D, *from these measurements, an average lumen diameter in millimeters is derived by the formula (a+b)/2, where* a *is the larger diameter and* b *is the smaller diameter. Similarly, a CSA in millimeters squared can be derived by the formula ($\pi \times a \times b/4$).*

treating it as an ellipse with major and minor axis diameters a and b, respectively (*Fig. 2D*). The luminal diameters were measured with a caliper function in two dimensions for each section, thus yielding the cross sectional area (CSA) of the parent vessel (4, 32), according to the formula ($\pi \times a \times b/4$). An average luminal diameter was computed as (a+b)/2 from the two measurements.

Points of measurement were selected at the following sites along the path of the parent vessel (*Fig. 3*): 1) 2 mm proximal to the stent (Point A), 2) 2 mm distal to the proximal struts (Point B), 3) midstent segment at the aneurysm neck (Point C), 4) 2 mm proximal to the distal struts (Point D), and 5) 2 mm distal to the distal struts (Point E). The same corresponding vessel points (A, B, D, and E) were chosen for measurement before treatment and after stent and coil deployment at the time of the original procedure and at the latest available angiographic follow-up study. Point C was measured after stent and coil deployment and at the latest follow-up time points because the absence of coils before treatment made the measurement point at the level of the aneurysm neck arbitrary and prone to variability.

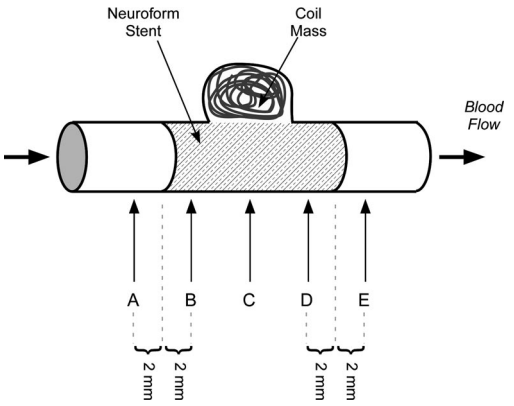


FIGURE 3. *Neuroform stent-coil schematic: points of measurement of parent vessel diameter. Point* A, *within the native parent vessel, 2 mm from the proximal edge of the stent. Point* B, *within the proximal stent segment, 2 mm from the proximal stent struts. Point* C, *the midstent segment at the aneurysm neck. Point* D, *the distal stent segment, 2 mm from the distal stent struts. Point* E, *the distal native parent vessel, 2 mm distal from the stent struts.*

Statistics

Differences between pretreatment, posttreatment, and latest follow-up diameter and CSA values were compared by use of paired *t* tests using the JMP software package, Version 5.0 (SAS Institute, Cary, NC). Correlation between clinical events and degree of luminal change and between patient characteristics, stent dimensions, duration at angiographic follow-up, and presence of luminal change were determined by use of a logistic regression model. Statistical significance was assumed at a value of $P < 0.05$.

RESULTS

Stent Location and Aneurysm Characteristics

A total of 16 Neuroform microstents were placed across 14 intracranial aneurysms in 14 patients (*Table 1*). Stent location was in the cavernous, paraclinoid, or ophthalmic segment of the internal carotid artery in 11 of 16 instances, the basilar artery to posterior cerebral artery P1 segment in 3 of 16 instances, the middle cerebral artery M1 to M2 segment in 1 of 16 instances, and at the origin of the posterior communicating artery segment of the internal carotid artery in 1 of 16 instances. In Patient 3, two stents were used in the "kissing" configuration to treat a basilar apex aneurysm with the two proximal stent segments in the basilar trunk and distal stent segments in each of the P1 segments of the posterior cerebral artery. Accordingly, Point C was chosen at the top of the basilar trunk facing the aneurysm. The measurements of Points A, B, and C were recorded as single observations, whereas the measurement of Points D and E were recorded as separate observations. In Patient 6, suboptimal stent positioning resulted in partial deployment of the proximal struts into the aneurysm neck; Points A and B were thus excluded from

Copyright © Congress of Neurological Surgeons. Unauthorized reproduction of this article is prohibited.

TABLE 1. Neuroform microstents placed across intracranial aneurysms[a]

Patient no.	Aneurysm location	No. of stents	Stent size (mm)	Time to follow-up (d)	Segments analyzed
1	CavICA	1	4.5 × 20	197	A, B, C, D, E
2	SupHypA	1	4.5 × 20	137	A, B, C, D, E
3	BasA	2	4 × 20 4 × 15	67	A, B, C, D (2), E (2)[b]
4	OpthA	1	4.5 × 20	74	A, B, C, D, E
5	OpthA	1	4 × 20	185	A, B, C, D, E
6	PComA	1	4 × 15	219	C, D, E[c]
7	PaCICA	1	4 × 15	154	A, B, C, D, E
8	CavICA	1	4.5 × 20	165	A, B, C, D, E
9	CavICA	2	4 × 20	157	A, B, C, D, E
10	BasA	1	3.5 × 20	14	A, B, C, D, E
11	OpthA	1	4 × 20	79	A, B, C, D, E
12	MCA	1	3 × 20	131	A, B, C, D, E
13	SupHypA	1	4 × 15	115	A, B, C, D, E
14	PaCICA	1	3.5 × 15	42	A, B, C, D, E

[a] CavICA, cavernous internal carotid artery; SupHypA, superior hypophyseal artery; BasA, basilar artery; OpthA, opthalmic artery; PComA, posterior communicating artery; PaCICA, paraclinoid internal carotid artery; MCA, middle cerebral artery.
[b] Each posterior cerebral artery was recorded as a separate observation for D and E.
[c] A and B not measured because the proximal stent was partially deployed within the aneurysm neck.

TABLE 2. Reductions in average cross-sectional area of parent vessel[a]

Parent vessel segment	Stenosis observed in	Average percent decrease in CSA (mean ± SEM)	Range (%)	Mean CSA change (mm^2)
A	10/13	5.6 ± 3.7	0.8–22.8	−0.62
B	12/13	19.2 ± 4.4	14.6–37.8	−2.40[b]
C	11/14	16.6 ± 5.2	1.8–55.8	−1.65[b]
D	13/15	18.0 ± 4.5	7.7–58.7	−1.47[b]
E	12/15	13.9 ± 7.4	11.6–52.8	−1.42[c]

[a] CSA, cross sectional area; SEM, standard error of the mean.
[b] $P < 0.01$.
[c] $P < 0.05$.

the analysis. In Patient 9, two stents were placed in a telescoping manner to bridge a very wide aneurysm neck. The total numbers of observations available for analysis were 13 at Point A, 13 at Point B, 14 at Point C, 15 at Point D, and 15 at Point E. Average time to follow-up was 124 ± 61 days (range, 14–219 d).

Stent diameter size ranged from 3 to 4.5 mm and length, either 15 or 20 mm. Stent size was selected on the basis of the initial diameter of the parent vessel in which the stent was to be deployed. A majority of the stents used (13/16, 81%) were either 4 or 4.5 mm in diameter.

Development of In-Stent Stenosis and Parent Vessel Remodeling at Follow-up

Qualitative evaluation of preliminary 2D-DSA angiographic follow-up images revealed the presence of discernible caliber changes at the level of the stent in certain patients (*Fig. 1*). To determine whether the stent-coil procedure itself had any impact on the parent vessel shape, measurements were made at Points A, B, D, and E on both the preprocedure and postprocedure 3D-DRA models. Point C was excluded from this phase of the analysis because the coil mass may produce a degree of stenosis on the parent vessel if the stent is deformed. Among the points analyzed, no statistically significant change in average vessel diameter was observed as a result of the stent-coil procedure at any of these points. The average diameter change at Point A was only 0.17 mm ($P < 0.20$), and for Points B, D, and E, it was 0.16, 0.06, and 0.16 mm ($P < 0.34$, $P < 0.58$, and $P < 0.21$), respectively.

In contrast, analysis of the 3D-DRA models obtained at the latest angiographic follow-up revealed statistically significant reductions in the average diameter of the parent vessel harboring the stent at several points (*Table 2*). The greatest degree of reduction of the average lumen

Copyright © Congress of Neurological Surgeons. Unauthorized reproduction of this article is prohibited.

diameter occurred within the proximal stent. At Point B, the mean decrease in diameter was 0.41 mm ($P < 0.001$). Smaller changes were seen at Points C, D, and E, with mean reductions of diameter of 0.32, 0.31, and 0.29 mm ($P < 0.011$, $P < 0.003$, and $P < 0.014$), respectively. No significant change was noted in the proximal native vessel, however. At Point A, proximal to the leading edge of the stent, the mean change in average diameter was a statistically insignificant 0.11 mm ($P < 0.13$) (*Fig. 4*).

We also measured changes in parent vessel luminal CSA (mm^2), which are more representative of clinical vessel luminal caliber. Average changes in CSA were evaluated at all points to determine an in vivo rate of stenosis. A decrease in luminal CSA was observed in 10 of 13 patients (77%) at Point A, 12 of 13 (92%) at Point B, 11 of 14 (79%) at Point C, 13 of 15 (87%) at Point D, and 12 of 15 (80%) at Point E. Some degree of stenosis was observed in at least one vessel segment in every patient (*Fig. 5*).

Proximal to the stent at Point A, we observed a nonsignificant reduction in CSA of 0.62 mm^2 ($P < 0.15$), corresponding to an average relative stenosis of 5.6 ± 3.7%. Corresponding to the reduction in average diameter, there was a 2.4-mm^2 narrowing at Point B, a 1.65-mm^2 narrowing at Point C, a 1.47-mm^2 narrowing at Point D, and a 1.42-mm^2 narrowing at Point E, corresponding to a 19.2 ± 4.4%, 16.6 ± 5.3%, 18.0 ± 4.5%, and 13.9 ± 7.4% relative stenosis ($P < 0.002$, $P < 0.006$, $P < 0.004$, and $P < 0.011$), respectively. The maximum percent change was also greater at Points B through E than that observed in the native proximal vessel at Point A. A theoretical estimate of the increased local hemodynamic resistance as a result of the decreased surface area was computed by assuming Poiseuille's equation. Because hemodynamic resistance is proportional to the inverse of the fourth power of the radius, it is proportional to the inverse square of the CSA. Accordingly, the theoretical increase in focal hemodynamic resistance at latest follow-up would be approximately 12%, 53%, 44%, 49%, and 35% at Points A, B, C, D, and E, respectively. The worst caliber reduction was seen with one patient experiencing a 59% reduction in CSA at Point D and another experiencing a 56% reduction in CSA at Point C. These correspond to an estimated 5.9- and 5.2-fold focal increased hemodynamic resistance, respectively. Conversely, the maximum stenosis experienced at Point A was only 23% (*Fig. 5*).

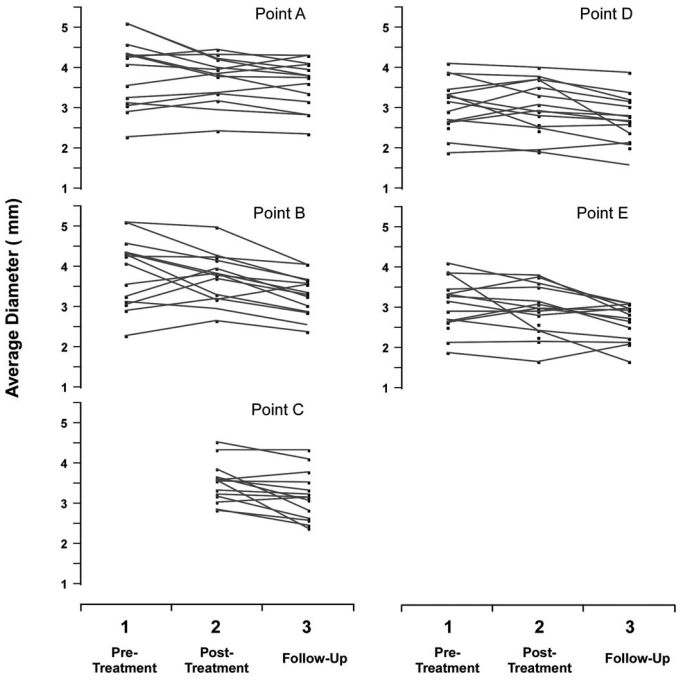


FIGURE 4. *Graphs showing time-dependent change in average vessel diameter. No significant change was observed in average diameter of the proximal native parent vessel at Point A. No significant change was observed in the proximal stent (B), distal stent (D), or distal parent vessel (E) between time Points 1 (pretreatment) and 2 (posttreatment). A significant decrease in average diameter (0.41 mm at B, 0.31 mm at D, and 0.29 mm at E; P < 0.001, 0.003, and 0.014, respectively) was seen at all three of these locations between time Points 2 (posttreatment) and 3 (follow-up). At the midstent segment (C), measurements were made only for time Points 2 and 3, in which a significant decrease in average parent vessel diameter (0.32 mm; P < 0.011) was detected.*

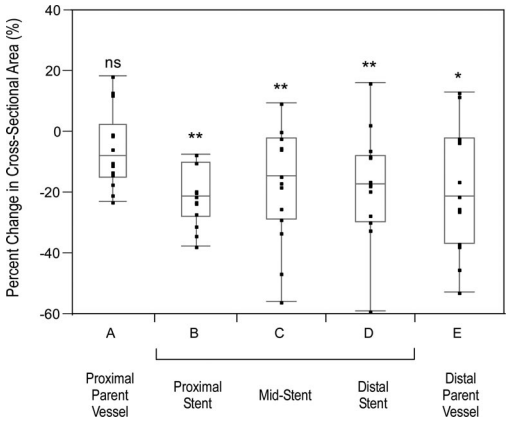


FIGURE 5. *Box plots demonstrating percent change in surface CSA. Boxplots demonstrate the median (*line*), 75th percentile (*box*), and 90th percentile (*bar*) values for percent reduction in CSA for Points A to E. *, P < 0.05; **, P < 0.01.*

Clinical Correlation

Covariates including age, presence of hypertension, size mismatch between the proximal and distal native vessel, aneurysm neck width, stent diameter, and stent/vessel diameter mismatch were analyzed for correlation with extent of luminal stenosis. No significant correlation was found at any of the measured points along the measured vessel and these covariates. In addition, no correlation was found between extent of luminal stenosis and time to latest angiographic follow-up. The statistical power of the present study to detect such correlations is limited.

There were no instances of embolic or ischemic stroke in this patient cohort. Delayed transient ischemic symptoms (transient ischemic attacks) were reported by five patients in the

Copyright © Congress of Neurological Surgeons. Unauthorized reproduction of this article is prohibited.

follow-up period, consisting of two episodes of visual changes, two episodes of facial paresthesias, and one episode of motor weakness in the cerebral territory supplied by the stented segment. No correlation was found between the degree of CSA reduction and clinical events in this patient cohort.

DISCUSSION

The Neuroform stent offers several theoretical advantages over traditional coronary stents with respect to the potential for development of neointimal hyperplasia. First, this is a self-expanding stent with an atraumatic deployment system and a low outward radial force of only 9 to 10 mm Hg, which is similar to the physiological force of the native vessel (2), thereby limiting the tensile stress imposed on the parent vessel wall. This low radial force permits deployment into size-mismatched vessels such as the basilar artery and P1 segment of the posterior cerebral artery or the internal carotid artery and the M1 segment of the middle cerebral artery without evidence of dilation of the smaller vessel (2, 7, 14). In its expanded form, the Neuroform stent is a segmented open-pore design with a cell size ranging from 2 to 2.5 French in diameter and relatively few strut–strut intersections to facilitate navigation and conformity to the parent vessel wall without straightening or affecting bifurcation angles; the strut thickness of the Neuroform stent is approximately one-third that of the Palmaz-Schatz coronary stent or Wallstent (9, 31). Endothelialization is said to occur within 30 days of stent deployment, and nitinol, the stent substrate material, is relatively inert and has been shown to compare favorably to stainless steel stents in extracranial carotid applications with regard to stenosis and clinical neurological outcome (24).

Despite these features, we observed a consistent reduction in average lumen diameter and surface CSA beginning in the proximal portion of the stent and extending to the native distal vessel by a process that did not seem to affect the proximal native vessel. No measurable effects on the vascular lumen were observed when the preprocedure was compared with the postprocedure luminal dimensions, and thus it seems unlikely that the intimal trauma imparted by stent deployment is the only source of the proliferative response observed here. In a large number of patients, the end-tines of the Neuroform stent, which were seen to be intraluminal at the end of the initial stent-coil procedure, were noted to be embedded within the vessel wall and no longer intraluminal.

Stent deployment evolved to counter restenosis after primary balloon angioplasty of coronary atherosclerosis, with prospective randomized trials showing lower rates of restenosis when stenting was added to balloon angioplasty (12, 15, 29, 34). This was accompanied by higher rates of subacute thrombosis within implanted stents (12), and in some animal studies, neointimal lesions arising in stented vascular segments were up to four times greater than those caused by balloon angioplasty alone (11, 20, 28). In-stent stenosis may be the result of endothelial or smooth muscle cell migration and proliferation and extracellular matrix deposition. The short-term response of the vessel wall to stent angioplasty involves infiltration with macrophages and polymorphonuclear leukocytes, with the number of infiltrating cells being correlated to the degree of intimal hyperplasia. The degree of neointimal hyperplasia is highly dependent on a number of arterial-wall, stent-delivery, and biomechanical factors, by mechanisms that remain poorly understood (6, 11, 20) but that have been successfully attenuated by the current generation of paclitaxel- and sirolimus-eluting coronary stents. Endovascular intervention can be traumatic to the vascular endothelium, resulting in microscopic focal mural thrombus within 1 to 3 days of stenting (26). Although thrombus formation has been linked to neointimal formation, it can be inhibited with no effect on later events in arterial remodeling (11, 27). Accordingly, most stent protocols, including ours, rely on aggressive antiplatelet therapy and systemic anticoagulation to minimize thrombus formation, and although microscopic injury to the vessel wall may have been present, it is minor compared with that attributed to angioplasty, which was absent in the present study.

Stent characteristics such as radial force, stent profile in the delivery system, number of struts, number of strut intersections, stent porosity, and strut thickness can all affect the degree of endothelial denudation and strut penetration into the arterial wall after deployment. These factors may result in chronic irritation to the vascular wall structures beyond the initial acute injury posed by the intervention itself, and strut-induced vascular injury has been correlated with a prolonged inflammatory response in porcine, canine, and murine models (3, 28, 35). Late-phase arterial wall remodeling can also be attributed to the arterial response to structurally imposed changes in vessel morphology and hemodynamics. Stent placement may result in vessel deformation and dilation, which the vessel wall may counter by increased collagen and extracellular matrix deposition through the stent struts (11, 17). In addition, the struts of the stent disrupt the smooth hemodynamic shear stress to which the endothelial layer is exposed in the native state, causing a patchwork of luminal areas that become subjected to a lower shear stress with secondary flow (shear-stress shielding), a phenomenon that itself may be a contributor to the intimal response seen here (19). It would be expected that such a phenomenon would be minimized in the case of the Neuroform stent, given its thin struts compared with other coronary balloon-mounted stents.

The power of this study to identify significant predictors of intimal hyperplasia after Neuroform stent deployment is somewhat limited. Intimal proliferation has been observed after angioplasty/stenting of intracranial atherosclerotic lesions with similar intracranial stents, but the implantation of a stent into an otherwise intact parent vessel at the site of an aneurysm represents a different biological process than implantation into a diseased atherosclerotic section of vessel (16, 23, 33). Recently, Fiorella et al. (13) reported on a case of Neuroform in-stent stenosis that resulted in clinically symptomatic middle cerebral artery stenosis, eventually necessitating bypass surgery. In contrast to the present series, the an-

Copyright © Congress of Neurological Surgeons. Unauthorized reproduction of this article is prohibited.

eurysm reported by Fiorella et al. had been filled with bioactive platinum coils coated with a polymer of polyglycolic acid and lactide (Matrix coil; Boston Scientific Inc.). A recent report by Lopes and Sani (21) provided the first postmortem histological study of a human cavernous carotid artery response to Neuroform stent implantation in the absence of coiling at the 3-month mark; the authors described only mild intimal thickening and a fibrocellular cap near the aneurysm neck, with complete endothelial coverage of the stent struts. It is not possible at this point to determine the relative histological contribution of smooth muscle cell proliferation, endothelial proliferation or migration, and extracellular matrix deposition to neointimal hyperplasia after Neuroform stent deployment.

To the best of our knowledge, this is the first study to use quantitative cerebral angiography using computer reconstructions of 3D-DRA data to evaluate CSA. Although concerns persist about the validity of quantifying neointimal formation by use of 2D-DSA versus intravascular ultrasound in coronary vessels, angiographic analysis shows correlation with histopathological section analysis (8, 10, 18, 25). Quantitative digital subtraction cerebral angiography takes advantage of three-dimensional reconstruction capabilities and the elimination of motion artifact in the intubated paralyzed patient. Furthermore, reconstructed 3-D-DRA images show only the vascular lumen; therefore, it is easy to evaluate detailed morphological characteristics of vessels and aneurysms via a three-dimensional vascular survey or "virtual angioscopy" (30, 32). Shaded surface display reconstruction provides the truest estimation of the vascular lumen, although overestimation of the CSA of aneurysm neck size of an intracavernous aneurysm secondary to bony artifact has been described (4).

A number of internal controls exist in our study suggesting that the decrease in luminal CSA is a real phenomenon. No significant difference in CSA was observed at any time within the proximal native vascular segment, nor was a significant change in luminal diameter observed after the procedure. Despite the moderate angiographic degree of CSA reduction observed here, there was no significant correlation with any clinical sequelae. In this patient cohort, no embolic or ischemic strokes have occurred within the vascular distribution supplied through the Neuroform stent. Five transient ischemic events have been reported during the follow-up period, consisting of visual changes, motor weakness, and sensory paresthesias, but no significant difference in CSA was observed in this group compared with those patients who did not experience transient ischemic attacks.

CONCLUSION

When measured by high-resolution 3D-DRA with reconstruction, statistically, but not clinically, significant in-stent stenosis was detected in patients treated with Neuroform stent–mediated coil embolization. Although this in-stent stenosis has been asymptomatic in this patient cohort, longer-term imaging and clinical and histopathological correlation will be needed to determine whether this is a benign self-limiting remodeling process or a more concerning progressive clinically significant arteriopathy.

REFERENCES

1. Albuquerque FC, Spetzler RF, Zabramski JM, McDougall CG: Effects of three-dimensional angiography on the coiling of cerebral aneurysms. **Neurosurgery** 51:596–605, 2002.
2. Alfke K, Straube T, Dorner L, Mehdorn HM, Jansen O: Treatment of intracranial broad-neck aneurysms with a new self-expanding stent and coil embolization. **AJNR Am J Neuroradiol** 25:584–591, 2004.
3. Andersen HR, Maeng M, Thorwest M, Falk E: Remodeling rather than neointimal formation explains luminal narrowing after deep vessel wall injury: Insights from a porcine coronary (re)stenosis model. **Circulation** 93:1716–1724, 1996.
4. Anxionnat R, Bracard S, Ducrocq X, Trousset Y, Launay L, Kerrien E, Braun M, Vaillant R, Scomazzoni F, Lebedinsky A, Picard L: Intracranial aneurysms: Clinical value of 3D digital subtraction angiography in the therapeutic decision and endovascular treatment. **Radiology** 218:799–808, 2001.
5. Anxionnat R, Bracard S, Macho J, Da Costa E, Vaillant R, Launay L, Trousset Y, Romeas R, Picard L: 3D angiography: Clinical interest—First applications in interventional neuroradiology. **J Neuroradiol** 25:251–262, 1998.
6. Bauters C, Isner JM: The biology of restenosis. **Prog Cardiovasc Dis** 40:107–116, 1997.
7. Benitez RP, Silva MT, Klem J, Veznedaroglu E, Rosenwasser RH: Endovascular occlusion of wide-necked aneurysms with a new intracranial microstent (Neuroform) and detachable coils. **Neurosurgery** 54:1359–1368, 2004.
8. Blasini R, Neumann FJ, Schmitt C, Bokenkamp J, Schomig A: Comparison of angiography and intravascular ultrasound for the assessment of lumen size after coronary stent placement: Impact of dilation pressures. **Cathet Cardiovasc Diagn** 42:113–119, 1997.
9. Broadbent LP, Moran CJ, Cross DT 3rd, Derdeyn CP: Management of neuroform stent dislodgement and misplacement. **AJNR Am J Neuroradiol** 24:1819–1822, 2003.
10. Bruining N, Sabate M, de Feyter PJ, Kay IP, Ligthart J, Disco C, Kutryk MJ, Roelandt JR, Serruys PW: Quantitative measurements of in-stent restenosis: A comparison between quantitative coronary ultrasound and quantitative coronary angiography. **Catheter Cardiovasc Interv** 48:133–142, 1999.
11. Edelman ER, Rogers C: Pathobiologic responses to stenting. **Am J Cardiol** 81:4E–6E, 1998.
12. Erbel R, Haude M, Hopp HW, Franzen D, Rupprecht HJ, Heublein B, Fischer K, de Jaegere P, Serruys P, Rutsch W, Probst P: Coronary-artery stenting compared with balloon angioplasty for restenosis after initial balloon angioplasty. Restenosis Stent Study Group. **N Engl J Med** 339:1672–1678, 1998.
13. Fiorella D, Albuquerque FC, Deshmukh VR, McDougall CG: In-stent stenosis as a delayed complication of neuroform stent-supported coil embolization of an incidental carotid terminus aneurysm. **AJNR Am J Neuroradiol** 25:1764–1767, 2004.
14. Fiorella D, Albuquerque FC, Han P, McDougall CG: Preliminary experience using the Neuroform stent for the treatment of cerebral aneurysms. **Neurosurgery** 54:6–17, 2004.
15. Fischman DL, Leon MB, Baim DS, Schatz RA, Savage MP, Penn I, Detre K, Veltri L, Ricci D, Nobuyoshi M, Cleman M, Heuser R, Almond D, Teirstein PS, Fish RD, Colombo A, Brinker J, Moses J, Shaknovich A, Hirshfeld J, Bailey S, Ellis S, Rake R, Goldberg S: A randomized comparison of coronary-stent placement and balloon angioplasty in the treatment of coronary artery disease. Stent Restenosis Study Investigators. **N Engl J Med** 331:496–501, 1994.
16. Gomez CR, Orr SC: Angioplasty and stenting for primary treatment of intracranial arterial stenoses. **Arch Neurol** 58:1687–1690, 2001.
17. Holmes DR Jr, Schwartz RS, Webster MW: Coronary restenosis: What have we learned from angiography? **J Am Coll Cardiol** 17:14B–22B, 1991.

Copyright © Congress of Neurological Surgeons. Unauthorized reproduction of this article is prohibited.

18. Kjelsberg MA, Seifert P, Edelman ER, Rogers C: Design-dependent variations in coronary stent stenosis measured as precisely by angiography as by histology. **J Invasive Cardiol** 10[Suppl B]:3B–11B, 1998.
19. LaDisa JF Jr, Olson LE, Guler I, Hettrick DA, Audi SH, Kersten JR, Warltier DC, Pagel PS: Stent design properties and deployment ratio influence indexes of wall shear stress: A three-dimensional computational fluid dynamics investigation within a normal artery. **J Appl Physiol** 97:416–430, 2004.
20. Libby P, Tanaka H: The molecular bases of restenosis. **Prog Cardiovasc Dis** 40:97–106, 1997.
21. Lopes D, Sani S: Histological postmortem study of an internal carotid artery aneurysm treated with the Neuroform stent. **Neurosurgery** 56:E416, 2005.
22. Lylyk P, Cohen JE, Ceratto R, Ferrario A, Miranda C: Endovascular reconstruction of intracranial arteries by stent placement and combined techniques. **J Neurosurg** 97:1306–1313, 2002.
23. Mori T, Kazita K, Chokyu K, Mima T, Mori K: Short-term arteriographic and clinical outcome after cerebral angioplasty and stenting for intracranial vertebrobasilar and carotid atherosclerotic occlusive disease. **AJNR Am J Neuroradiol** 21:249–254, 2000.
24. Mukherjee D, Kalahasti V, Roffi M, Bhatt DL, Kapadia SR, Bajzer C, Reginelli J, Ziada KM, Hughes K, Yadav JS: Self-expanding stents for carotid interventions: Comparison of nitinol versus stainless-steel stents. **J Invasive Cardiol** 13:732–735, 2001.
25. Prati F, Pawlowski T, Sommariva L, Labellarte A, Manzoli A, Boccanelli A, Motolese M: Intravascular ultrasound and quantitative coronary angiography assessment of late in-stent restenosis: In vivo human correlation and methodological implications. **Catheter Cardiovasc Interv** 57:155–160, 2002.
26. Rogers C, Welt FG, Karnovsky MJ, Edelman ER: Monocyte recruitment and neointimal hyperplasia in rabbits: Coupled inhibitory effects of heparin. **Arterioscler Thromb Vasc Biol** 16:1312–1318, 1996.
27. Schafer K, Konstantinides S, Riedel C, Thinnes T, Muller K, Dellas C, Hasenfuss G, Loskutoff DJ: Different mechanisms of increased luminal stenosis after arterial injury in mice deficient for urokinase- or tissue-type plasminogen activator. **Circulation** 106:1847–1852, 2002.
28. Schwartz RS, Huber KC, Murphy JG, Edwards WD, Camrud AR, Vlietstra RE, Holmes DR: Restenosis and the proportional neointimal response to coronary artery injury: Results in a porcine model. **J Am Coll Cardiol** 19:267–274, 1992.
29. Serruys PW, de Jaegere P, Kiemeneij F, Macaya C, Rutsch W, Heyndrickx G, Emanuelsson H, Marco J, Legrand V, Materne P, Belardi J, Sigwart U, Colombo A, Goy JJ, van den Heuvel P, Delcan J, Morel M: A comparison of balloon-expandable-stent implantation with balloon angioplasty in patients with coronary artery disease. Benestent Study Group. **N Engl J Med** 331:489–495, 1994.
30. Sugahara T, Korogi Y, Nakashima K, Hamatake S, Honda S, Takahashi M: Comparison of 2D and 3D digital subtraction angiography in evaluation of intracranial aneurysms. **AJNR Am J Neuroradiol** 23:1545–1552, 2002.
31. Tanaka N, Martin JB, Tokunaga K, Abe T, Uchiyama Y, Hayabuchi N, Berkefeld J, Rufenacht DA: Conformity of carotid stents with vascular anatomy: Evaluation in carotid models. **AJNR Am J Neuroradiol** 25:604–607, 2004.
32. Unno N, Mitsuoka H, Takei Y, Igarashi T, Uchiyama T, Yamamoto N, Saito T, Nakamura S: Virtual angioscopy using 3-dimensional rotational digital subtraction angiography for endovascular assessment. **J Endovasc Ther** 9:529–534, 2002.
33. Vallee JN, Pierot L, Bonafe A, Turjman F, Flandroy P, Berge J, Rodesch G, Bracard S: Endovascular treatment of intracranial wide-necked aneurysms using three-dimensional coils: Predictors of immediate anatomic and clinical results. **AJNR Am J Neuroradiol** 25:298–306, 2004.
34. Versaci F, Gaspardone A, Tomai F, Crea F, Chiariello L, Gioffre PA: A comparison of coronary-artery stenting with angioplasty for isolated stenosis of the proximal left anterior descending coronary artery. **N Engl J Med** 336:817–822, 1997.
35. Wakhloo AK, Schellhammer F, de Vries J, Haberstroh J, Schumacher M: Self-expanding and balloon-expandable stents in the treatment of carotid aneurysms: An experimental study in a canine model. **AJNR Am J Neuroradiol** 15:493–502, 1994.
36. Wanke I, Doerfler A, Schoch B, Stolke D, Forsting M: Treatment of wide-necked intracranial aneurysms with a self-expanding stent system: Initial clinical experience. **AJNR Am J Neuroradiol** 24:1192–1199, 2003.

COMMENTS

Hoit and Malek report their results with the application of three-dimensional rotational angiography for quantification of cross-sectional area loss in the parent vessel and the implications for patients harboring cerebral aneurysms treated with Neuroform stent-assisted coiling (Boston Scientific/Target, Fremont, CA). The authors have meticulously conducted this study. Overall, they found a reduction in the cross-sectional area of the vessel throughout the stented segment, with a greatest mean stenosis of 19% at the proximal edge of the stent (Point B).

Cautious interpretation of these results is warranted to avoid drawing misleading conclusions. The authors mention that "in-stent stenosis" was present in all cases in at least one of the points measured. As they point out, this finding was of statistical significance with no clinical significance, in that none of their patients developed symptoms or required additional treatment. Any stent implantation will lead to a reduction in cross-sectional area because of the apposition of the stent to the vessel lumen, plus the neointimal proliferation produced as part of the healing response induced by the presence of the stent. As demonstrated in an in vivo intracranial stent model, the reduction in cross-sectional area is proportional to the vessel diameter, with larger losses occurring in smaller vessels (3, 4).

Clinically significant in-stent stenosis after Neuroform stent implantation has been reported (1), but the incidence of such events is low, considering the large number of stents implanted for aneurysm treatment. For instance, in our long-term evaluation of stent-assisted coiling for intracranial aneurysms using balloon-mounted (coronary) stents, we found no angiographic evidence of in-stent stenosis in 21 patients treated evaluation (mean follow-up, 4.9 yr) (2). Although the authors' conclusion points to the possibility of this process being a more concerning, progressive type of clinically significant arteriopathy, our experience with intracranial stents for aneurysms leads us to believe that the cross-sectional area reduction noticed by the authors is part of the vascular response to the stent, most likely constituting a self-limiting process. The clinical implications of their findings remain to be determined by further studies of intracranial Neuroform stent implantation with longer-term follow-up.

Ricardo A. Hanel
L. Nelson Hopkins
Buffalo, New York

1. Fiorella D, Albuquerque FC, Deshmukh VR, McDougall CG: In-stent stenosis as a delayed complication of Neuroform stent-supported coil embolization of an incidental carotid terminus aneurysm. **AJNR Am J Neuroradiol** 25:1764–1767, 2004.
2. Hanel RA, Bendok BR, Boulos AS, Levy EI, Kim SH, Hartney M, Qureshi AI, Guterman LR, Hopkins LN: Stent assisted coiling for intracranial aneurysms: Long-term clinical and angiographic follow-up. Presented at the Brazilian Meeting of Neurosurgery, Fortaleza, Brazil. September, 2002.
3. Levy EI, Boulos AS, Hanel RA, Tio FO, Alberico RA, Fronckowiak MD, Nemes B, Paciorek AM, Guterman LR, Hopkins LN: In vivo model of intracranial stent implantation: a pilot study to examine the histological response of cerebral vessels after randomized implantation of heparin-coated and uncoated endoluminal stents in a blinded fashion. **J Neurosurg** 98:544–553, 2003.
4. Levy EI, Hanel RA, Howington JU, Nemes B, Boulos AS, Tio FO, Paciorek AM, Amlani S, Kagan-Hallett KS, Fronckowiak MD, Guterman LR, Hopkins LN: Sirolimus-eluting stents in the canine cerebral vasculature: A prospective, randomized, blinded assessment of safety and vessel response. **J Neurosurg** 100:688–694, 2004.

Copyright © Congress of Neurological Surgeons. Unauthorized reproduction of this article is prohibited.

Malek and Hoit describe their three-dimensional angiographic analysis of in-stent stenosis in patients with wide-necked intracranial aneurysms who have undergone Neuroform stent-supported coiling. This study elegantly describes and quantifies a perplexing radiographic and clinical sequela of stent-supported coil embolization. I suspect that, as we continue to use intracranial stents for the treatment of these lesions, we will see more instances of clinically significant in-stent stenosis. In fact, in our personal experience, we have witnessed this occurrence in a number of patients. While some of these patients have remained asymptomatic, others have required angioplasty through the stented segment, bypass surgery, or both. The etiology of in-stent stenosis has yet to be determined. Although the theory of intimal hyperplasia is attractive, it has yet to be proved conclusively, specifically in relation to the Neuroform stent and its applications. This report adds to our growing understanding of the efficacy and potential complications of this endovascular device.

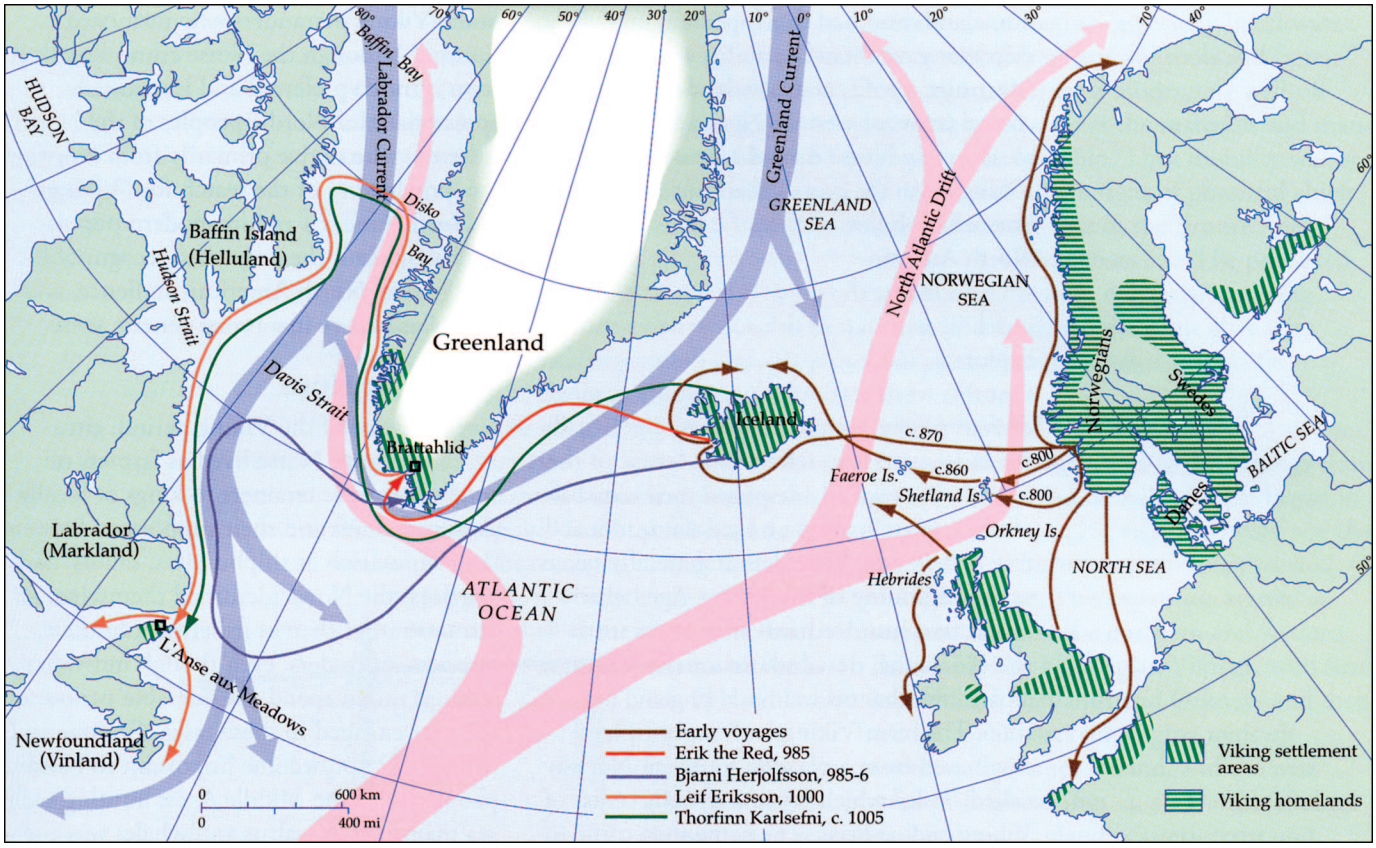
Felipe C. Albuquerque
Phoenix, Arizona

The authors present a very detailed retrospective analysis of a series of patients with aneurysms treated with the use of the Neuroform stent. Unlike stent placement elsewhere in the body, placement of the Neuroform stent for the purpose of performing stent-assisted coil embolization does not require an associated angioplasty or balloon expandable method of deployment. Until now, it was hypothesized that the Neuroform stent would be associated with a low rate of in-stent stenosis owing to a potentially reduced healing response compared with arteries stented with balloon expandable stents or those in which an angioplasty is also performed.

Using digital measuring tools incorporated in two- and three-dimensional angiography equipment, the authors have analyzed the healing response and resultant in-stent stenosis associated with the Neuroform stent. Their methoda will be extremely useful to other investigators in future analyses of new stents and these data will serve as their baseline for comparison.

Donald W. Larsen
Los Angeles, California

Norse voyages in the North Atlantic. (Courtesy of the Museum of Natural History, Smithsonian Institution, Washington).



Copyright © Congress of Neurological Surgeons. Unauthorized reproduction of this article is prohibited.